Available online at www.sciencedirect.com
SCIENCE DIRECT®
Journal of Solid State Chemistry 179 (2006) 522–531
JOURNAL OF SOLID STATE CHEMISTRY
www.elsevier.com/locate/jssc

Structural, microstructural and vibrational characterization of apatite-type lanthanum silicates prepared by mechanical milling

E. Rodríguez-Reyna[a], A.F. Fuentes[a,*], M. Maczka[b], J. Hanuza[b,c], K. Boulahya[d], U. Amador[e]

[a]*Cinvestav-Saltillo, Apartado Postal 663, 25000-Saltillo, Coahuila, Mexico*
[b]*Institute of Low Temperature and Structure Research, Polish Academy of Sciences, P.O. Box 1410, 50-950 Wroclaw 2, Poland*
[c]*Department of Bioorganic Chemistry, Faculty of Engineering and Economics, University of Economics, Wroclaw, Poland*
[d]*Departamento de Química Inorgánica, Facultad de Ciencias Químicas, Universidad Complutense, 28040-Madrid, Spain*
[e]*Departamento de Ciencias Químicas, Facultad de Farmacia, Universidad San Pablo CEU, 28668-Boadilla del Monte, Madrid, Spain*

Received 9 September 2005; received in revised form 1 November 2005; accepted 6 November 2005
Available online 13 December 2005

Abstract

Apatite-type lanthanum silicates have been successfully prepared at room temperature by dry milling hexagonal A-La_2O_3 and either amorphous or low cristobalite SiO_2. Milling a stochiometric mixture of these chemicals in a planetary ball mill with a moderate rotating disc speed (350 rpm), allows the formation of the target phase after only 3 h although longer milling times are needed to eliminate all SiO_2 and La_2O_3 traces. Thus, the mechanically activated chemical reaction proceeds faster when using amorphous silica instead of low cristobalite as silicon source and pure phases are obtained after only 9 and 18 h, respectively. As obtained powder phases are not amorphous and show an XRD pattern as well as IR and Raman bands characteristic of the lanthanum silicate. The domain size of the as-prepared phases varies gradually with the temperature of post-milling thermal treatment with activation energies of about 26(8) and 52(10) kJ mol^{-1} K^{-1} for the apatites obtained from amorphous silica and low-cristobalite, respectively. These values suggest crystallite growth to be favored when using amorphous silica as reactant.

Keywords: Apatite-type lanthanum silicates; Oxide ion conductors; Band analysis; Mechanochemical synthesis; IR and Raman spectra

1. Introduction

The conventional powder synthesis technology consisting of long firing cycles at high temperatures, presents some disadvantages such as poor control of morphology and particle size as well as phase and stoichiometric heterogeneities. Over the years, several alternatives such as co-precipitation or the sol–gel route have been proposed to increase reaction rates or to decrease reaction temperatures although more than often, they also require of thermal treatments, typically at temperatures around 800 °C, for the crystallization of the desired product. Mechanical milling, conceived initially to synthesize nanocrystalline metals and powder alloys [1], has been also recently used in ceramics to for example, synthesize novel crystalline phases or to produce a fine dispersion of second-phase particles and extended solid solutions. We describe in this paper a room-temperature method for preparing apatite-type lanthanum silicate, a solid oxide ion conductor, by mechanically milling stochiometric mixtures of the constituent oxides, La_2O_3 and SiO_2. Solid solutions of general formula $La_{10-x}(SiO_4)_6O_{3-1.5x}$ have recently gained considerable attention because of their high ionic conductivity at low temperatures (e.g. 0.01 S cm^{-1} at 700 °C) [2]. Studied originally by Nakayama and co-workers [2–4] and despite their promising performances, their application has been hindered by the very high temperatures (1200–1600 °C) and long firing cycles needed for their synthesis and sintering [5]. A sol–gel approach starting from stoichiometric mixtures of tetraethoxysilane (TEOS) and La_2O_3 or hydrated lanthanum nitrate has been also used. However, this method needs also a final thermal treatment at temperatures between 800 and 1000 °C to promote the

*Corresponding author. Fax: +52 84 44 38 96 10.
E-mail address: antonio.fernandez@cinvestav.edu.mx (A.F. Fuentes).

0022-4596/$ - see front matter © 2005 Elsevier Inc. All rights reserved.
doi:10.1016/j.jssc.2005.11.008

formation of the target phase [6,7]. A combination of mechanical milling a mixture of La_2O_3 and amorphous silica gel and a thermal treatment of the amorphous precursor material obtained at 1000 °C, have been also proposed to prepare these silicates [8].

We will present in this work a rapid method to obtain crystalline apatite-type lanthanum silicates including the evaluation of two different silicon sources (amorphous and low cristobalite SiO_2). We will also present an analysis of the structural and microstructural evolution of the as-prepared powder phases with the temperature of post-milling thermal treatment by combining XRD, electron microscopy and IR and Raman spectroscopy.

As neutron diffraction studies carried out in the $La_{10-x}(SiO_4)_6O_{3-1.5x}$ apatite series, have shown that hexagonal single phases are obtained only in a narrow compositional range (SiO_2:La_2O_3 molar ratios between 9:7 and 5:4) [9], all mixtures studied in this work were prepared with a 5:4 molar ratio (SiO_2:La_2O_3) corresponding to a reaction product with a chemical formula of $La_{9.60}(SiO_4)_6O_{2.4}$.

2. Experimental procedure

Stoichiometric mixtures of La_2O_3 (Aldrich Chem. Inc. 99.99%) and amorphous silica (Aldrich Chem. Inc. 99.8%; particle size = 0.014 μm; surface area = $200 \pm 25\,m^2/g$) or low cristobalite SiO_2 (Fluka 99.95%) in a 5:4 (SiO_2:La_2O_3) molar ratio, were weighed and placed in 125 ml zirconia containers together with six 20 mm diameter zirconia balls (mass ≈24 g) as to keep the balls-to-powder mass ratio equal to 10:1. In a typical experiment, a 15 g batch of reactants were dry milled in air in a Retsch PM400 planetary ball mill by using a rotating disc speed of 350 rpm with reversed rotation every 20 min. Phase evolution with milling time was followed by using X-ray powder diffraction in a Philips X'pert diffractometer using Ni-filtered Cu$K\alpha$ radiation ($\lambda = 1.5418$ Å).

The structural and microstructural features of the as-prepared materials were obtained from precise diffraction data obtained on a Bruker D8 high-resolution X-ray powder diffractometer, using monochromatic Cu$K\alpha_1$ ($\lambda = 1.5406$ Å) radiation obtained with a germanium primary monochromator, and equipped with a position sensitive detector (PSD) MBraun PSD-50M. The measured angular range, the step size and counting times were selected to ensure enough resolution (the step size should be at least, 1/10 of the fwhms) and statistics. The instrumental contribution to line broadening was evaluated using NIST LaB_6 standard reference material (SRM 660a; $\mu = 1138\,cm^{-1}$, linear absorption coefficient for Cu$K\alpha_1$ radiation). The structural refinements were carried out by the Rietveld method using the FullProf program [10]; in some cases, a severe microstructural contribution to the profile must be considered. In these cases, we have undertaken the refinement of the structures of our materials taking into account, simultaneously, the effects of their microstructure on the diffraction patterns. We have applied a phenomenological approach using a capability of the FullProf program which allows some of the peaks to be described by their own breadths and shapes, as well as small displacements from their positions calculated from the average unit cell. Prior to the structure refinements, a pattern matching without structural model was performed. This procedure allows obtaining suitable profile parameters, including the breadths, shapes and displacements of those reflections with relevant microstructural contributions. Then, the structural model is refined keeping constant the profile parameters. If needed, along the refinements some of these profile parameters are allowed to vary; but at the final steps of the refinements they are kept constant. The refinements were stable provided the number of refined parameters describing the structural model was low enough to obtain an adequate peaks-to-parameters ratio. To ensure this, an overall isotropic thermal factor (ITF) is used for all the atoms in the structure. The fitting process was finished when convergence is reached. Finally, the study of the microstructure of the samples was performed by the two-step procedure proposed by Langford [11,12] and Louër [13].

The samples were examined by scanning electron microscopy (SEM) in a Philips XL30 ESEM microscope equipped with an EDAX Inc. energy-dispersive X-ray detector for microanalysis. A JEOL 3000 FEG electron microscope was used for transmission electron microscopy studies (TEM) to determine the local composition (using energy-dispersive X-ray spectroscopy (EDS) with an INCA analyzer system attached to the microscope) and to study the samples crystallinity.

Polycrystalline infrared spectra were measured with a Biorad 575C FT-IR spectrometer as KBr pellets in the mid-IR region and in Nujol suspension in the far-IR region. Raman spectra were recorded with a Bruker FT-Raman RFS 100/S spectrometer. Excitation was performed with a YAG:Nd^{3+} laser. IR and Raman spectra were recorded with a spectral resolution of $2\,cm^{-1}$.

3. Results and discussion

3.1. X-ray diffraction

Fig. 1b and c show the XRD patterns of both reaction mixtures after different milling times, 1, 3, 6, 9 and 18 h. As a reference, Fig. 1a shows the XRD pattern of the starting mixture containing α-cristobalite SiO_2 where the only reflections observed are those characteristic of a hexagonal form of La_2O_3 and the silicon dioxide most intense reflection, the {101} line at 21.868° (2θ). The starting XRD pattern of the mixture containing amorphous SiO_2 is similar to the one presented but for the absence of any reflection due to silicon dioxide. The two main polymorphs of lanthanum sesquioxide are a cubic C-La_2O_3 form (SG Ia3), stable from room temperature up to around 500 °C, and a hexagonal A-La_2O_3 form (SG $P\bar{3}m1$), from 500 to

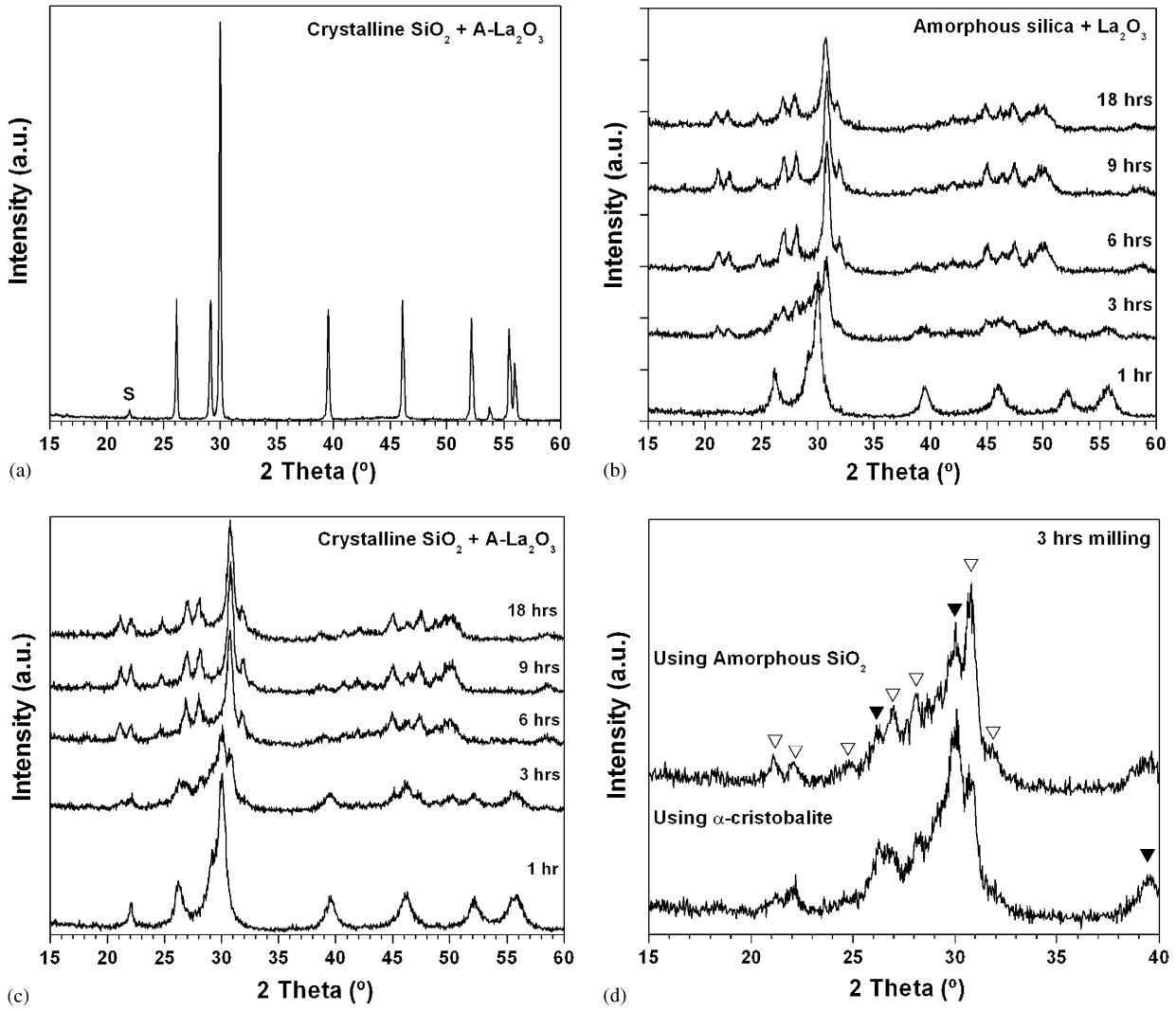

Fig. 1. XRD patterns showing: (a) the starting (α-cristobalite $SiO_2 + A\text{-}La_2O_3$) powder mixture; (b) the evolution of the (amorphous $SiO_2 + A\text{-}La_2O_3$); (c) (α-cristobalite $SiO_2 + A\text{-}La_2O_3$) mixtures with milling time; and (d) a comparison between both mixtures after milling for 3 h where (▼) and (▽) designate characteristic reflections of $A\text{-}La_2O_3$ and lanthanum silicate, respectively.

2000 °C. Two additional high temperature crystalline forms of La_2O_3 are also known, a cubic ($X\text{-}La_2O_3$) and hexagonal ($H\text{-}La_2O_3$). Our lanthanum source seems to consist only of $A\text{-}La_2O_3$ and all the reflections observed in Fig. 1a could be indexed according to the structural model given by Koehler and Wollan [14] for the $A\text{-}La_2O_3$ polymorph. After milling for 1 h both mixtures present similar XRD patterns but for the presence of the main α-cristobalite SiO_2 reflection. The effect of this initial milling period is much more pronounced in $A\text{-}La_2O_3$ whose characteristic reflections present a significant decrease in intensity (>75%) and peak broadening when compared with those of the initial powder, consequence of a considerable decrease in particle size and the introduction of a large number of crystal defects on milling. Thus, the intensity ratio between the most intense reflections of both $A\text{-}La_2O_3$ and α-cristobalite, the {011} and {101}lines, respectively, changes from 30.6 in the starting mixture to 5.0 in that milled for 1 h. As the grinding time increases to 3 h, new reflections emerge in the 20–35° region (2θ), to the point that for example, the main reflection of $A\text{-}La_2O_3$, the {011} line at 29.97° (2θ), is no longer the most intense of the XRD pattern containing amorphous SiO_2. None of these new reflections could be assigned to any form of La_2O_3 or crystalline SiO_2 but to the hexagonal apatite-type lanthanum silicate (PDF 49-0443). Thus, for example the lines appearing at ≈30.7°, 21° and 22° (2θ) are identified, respectively, as the $\{3\bar{1}1\}$, {200} and $\{2\bar{1}1\}$ lines belonging to the lanthanum silicate. After milling for 6 h, the only reflections observed in both mixtures are those characteristic of the silicate. Further milling does not bring about important changes in the XRD patterns and even after milling for 18 h, the characteristic reflections of the apatite-type phase, are the only ones present. Therefore, milling a mixture of La_2O_3 and amorphous SiO_2 or α-cristobalite for 6 h at a moderate rotating disc speed, is enough to induce a chemical reaction and to obtain a product consisting primarily of an apatite-type lanthanum silicate. Is reaction equally fast and

complete in both mixtures? Judging from the XRD patterns obtained after milling for 3 h which are shown in detail in Fig. 1d, the unreacted amount of lanthanum oxide still remaining in the powder mixture at that point, seems to be larger in the one containing α-cristobalite. An interesting observation to point out is that both starting reagents and the product phase coexist together during the process. Therefore, the formation of the reaction product does not involve crystallization of the target phase from an amorphous matrix as observed in other systems. This point is further confirmed by using TEM; as Fig. 2a and b show, the as-milled samples are crystalline materials. Indeed, in Fig. 2a and b well-defined spots are clearly seen, corresponding to well-crystallized compounds.

To study the evolution of the as-prepared lanthanum silicates with temperature, different portions of both samples were fired at temperatures between 400 and 1000 °C and characterized as described in the Experimental section. As Fig. 3a and b show, firing the as-prepared powder phases at temperatures of up to 600 °C for 12 h do not bring about major changes in the characteristic XRD patterns of both mixtures. However, treating the milled powders at 800 and 1000 °C produces peaks with increasing intensity and decrease in peak broadening corresponding to better ordered samples. As stated above, the effect of heat treatment is not the crystallization of the apatite-like phase from an amorphous matrix, but the growth of the crystalline domain. Morphology of the milled powders is illustrated in Fig. 4. As evident from this SEM micrograph, the lanthanum silicate consists basically of two types of agglomerates/particles. The first ones are constituted by submicron size particles bonded into clusters and are typical of reaction products obtained by mechanochemical synthesis. There are also larger particles with well-defined and sharp edges indicating a relatively small damage during the milling process because of the moderate rotation

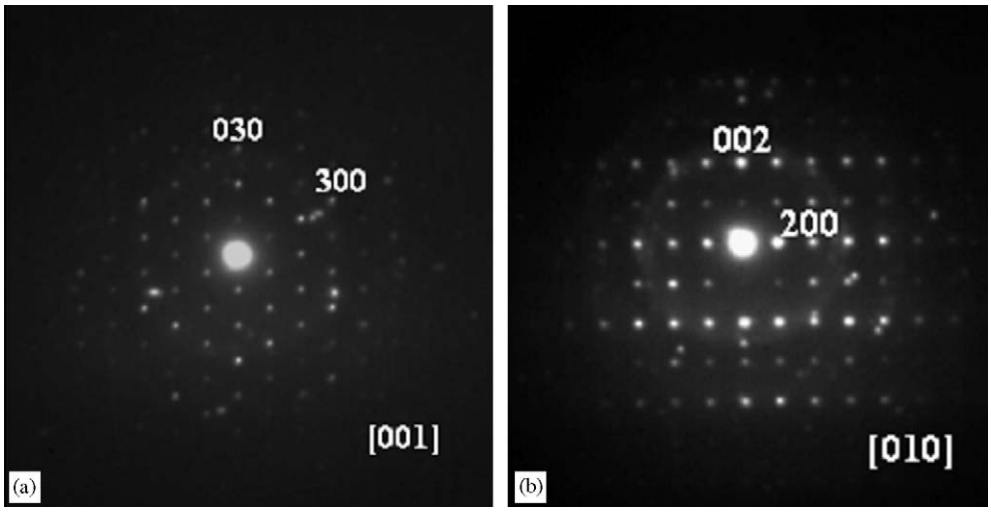

Fig. 2. (a) SAED pattern taken along [001] for the as-milled apatite-like sample prepared from amorphous silica; and (b) SAED pattern along [010] for the as-milled apatite-like sample prepared from α-cristobalite.

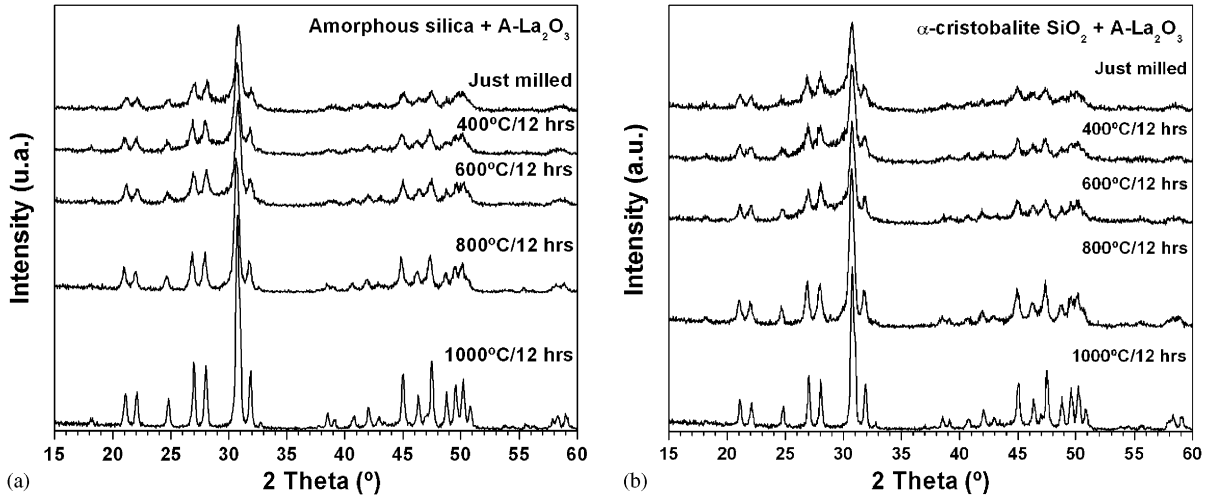

Fig. 3. Evolution of the as-prepared lanthanum silicates with temperature.

speed and the short milling time used. Microanalysis results show similar Si/La ratio for both types of particles.

3.2. Structure and microstructure

Fig. 5a and b show the graphic result of the fitting of the X-ray diffraction patterns corresponding to apatite-like compounds obtained by ball milling at RT for 9 h using amorphous silica as silicon source, and to a portion of this sample after a thermal treatment at 1000 °C for 12 h. Two points are evident from these figures: first, the samples consists of apatite-like materials and no extra peaks are observed; and second, the contribution of the microstructural features of the samples to the XRD patterns plays a decisive role in the structural refinement of most of these samples. This contribution has been taken into account in the refinement as described in the experimental section. At this point it must be remarked that X-ray diffraction techniques are no adequate to study structural features related to light atoms such as oxygen (or even silicon when heavy atoms like lanthanum are present); therefore in our structure refinements (Tables 1 and 2) we assumed that the oxygen array is complete and some extra oxygen is located at the tunnels according to the model proposed by León-Reina et al. [9] (see Fig. 6) and to fit the patterns of the most defective samples, the atomic parameters of oxygen atoms were not refined. Tables 1 and 2 also show some microstructural information obtained from Langford plots [11,12]. As observed in Tables 1 and 2, all the samples prepared present similar cell parameter, the difference of

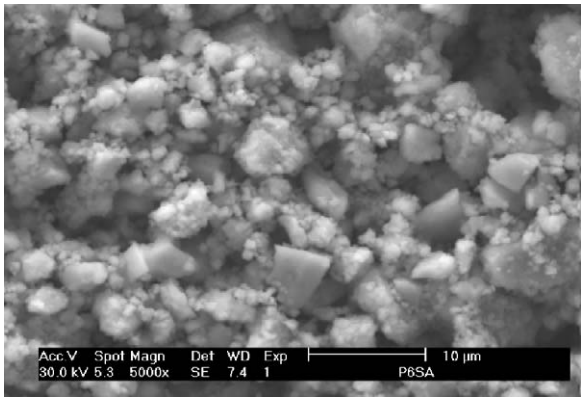

Fig. 4. A typical SEM micrograph obtained for the as-prepared lanthanum silicates.

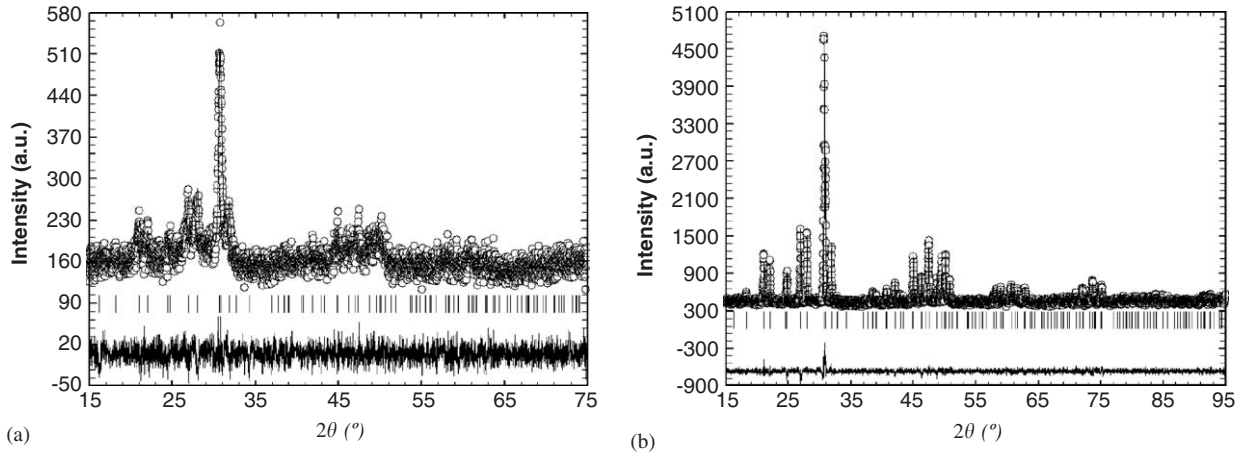

Fig. 5. (a) Experimental (points), calculated (solid line) and difference (bottom) X-ray diffraction patterns for as-milled apatite-like sample prepared from amorphous silica; and (b) experimental (points), calculated (solid line) and difference (bottom) X-ray diffraction patterns for a portion of the above sample after a thermal treatment at 1000 °C for 12 h.

Table 1
Selected structural and microstructural information of apatite-like samples prepared from amorphous silica as silicon source

Composition Treatment T (°C)/time (h)	$La_{9.42(1)}(SiO_4)_6O_{2.2(1)}$ 1200/12	$La_{9.50(1)}(SiO_4)_6O_{2.2(1)}$ 1000/12	$La_{9.25(1)}(SiO_4)_6O_{2.2}$ 800/12	$La_{9.5(1)}(SiO_4)_6O_{2.2}$ 600/12	$La_{9.5(1)}(SiO_4)_6O_{2.2}$ 400/12	$La_{9.5(1)}(SiO_4)_6O_{2.2}$ No treatment
a (Å)	9.7283(1)	9.7286(1)	9.7264(3)	9.7213(6)	9.720(1)	9.719(2)
c (Å)	7.1814(1)	7.1847(1)	7.1889(3)	7.1966(7)	7.197(1)	7.189(2)
R_B	0.0843	0.0295	0.0424	0.0423	0.044	0.0432
R_{wp}	0.0594	0.0522	0.0670	0.0916	0.0888	0.080
R_{exp}	0.0550	0.0449	0.0522	0.0849	0.0831	0.078
χ^2	1.18	1.35	1.65	1.16	1.14	1.03
$\langle D_{iso} \rangle$ (Å)	2950(350)	510(20)	450(8)	266(66)	148(19)	103(8)
e_{rms}	$2.5(5) \times 10^{-4}$	$4(3) \times 10^{-4}$	$4(2) \times 10^{-3}$	$6(1) \times 10^{-3}$	$4(3) \times 10^{-3}$	$6(3) \times 10^{-3}$

A complete structural information is available as supplementary material.

Table 2
Selected structural and microstructural information of apatite-like samples prepared from low cristobalite as silicon source

Composition Treatment T (°C)/time (h)	$La_{9.32(1)}(SiO_4)_6O_{2.2(1)}$ 1200/12	$La_{9.45(1)}(SiO_4)_6O_{2.2(1)}$ 1000/12	$La_{9.42(1)}(SiO_4)_6O_{2.2}$ 800/12	$La_{9.46(5)}(SiO_4)_6O_{2.2}$ 600/12	$La_{9.38(7)}(SiO_4)_6O_{2.2}$ 400/12	$La_{9.5(1)}(SiO_4)_6O_{2.2}$ No treatment
a (Å)	9.7262(1)	9.7284(2)	9.7255(7)	9.727(1)	9.7261(4)	9.719(2)
c (Å)	7.1852(1)	7.1845(2)	7.1930(5)	7.1948(8)	7.1896(4)	7.188(2)
R_B	0.0695	0.0677	0.0497	0.0336	0.0290	0.0432
R_{wp}	0.0584	0.0565	0.0818	0.0464	0.0376	0.080
R_{exp}	0.0499	0.0504	0.0788	0.0451	0.0362	0.078
χ^2	1.37	1.26	1.08	1.06	1.07	1.03
$\langle D_{iso} \rangle$ (Å)	3600(700)	390(10)	160(10)	140(11)	139(7)	121(20)
e_{rms}	$9(1) \times 10^{-5}$	$3(2) \times 10^{-4}$	$3(2) \times 10^{-3}$	$5(1) \times 10^{-3}$	$5(1) \times 10^{-3}$	$5(1) \times 10^{-3}$

A complete structural information is available as supplementary material.

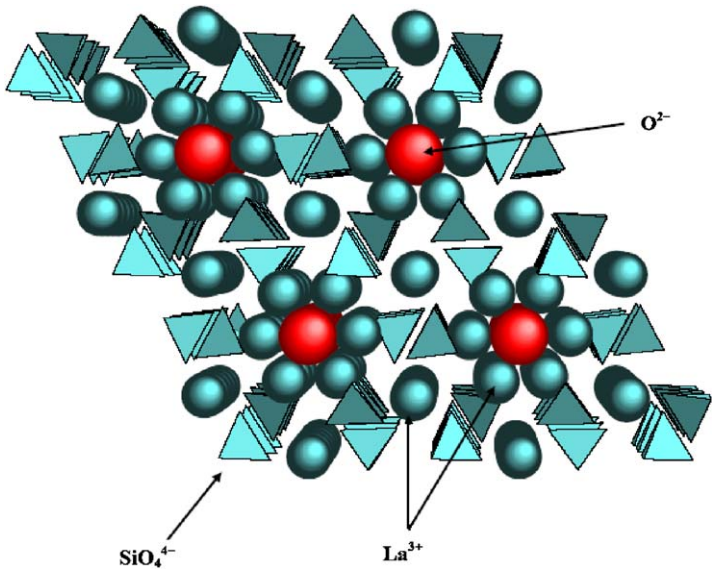

Fig. 6. Representation of the structure of apatite $La_{10-x}(SiO_4)_6O_{3-1.5x}$.

cell volume being about 0.2%. The compositions of all the samples are also similar, though XRD data seem to suggest slight differences in the lanthanum contents. Interestingly, the samples seem to be lanthanum-deficient since all mixtures studied in this work were prepared with a 5:4 molar ratio (SiO_2:La_2O_3) corresponding to a reaction product with a chemical formula of $La_{9.60}(SiO_4)_6O_{2.4}$. This could be related to the presence of small amounts of $La_2Zr_2O_7$ (Zr comes from the reaction containers made of zirconia) detected by SEM and TEM, that should be below 3–5% since this compound is not detected by XRD.

It is well established that mechanochemically prepared materials have a complex microstructure that cannot be accounted for by the conventional models. To study the microstructure of these compounds we have used the procedure proposed by Langford [12] and Louër [13]. As expected, due to the method of synthesis (high energy milling) the samples present significant residual microstrains and small crystallite size. According to Langford [11] and Halder and Wagner [15], the contributions to the integral breadth of strains and domain size can be separated using

$$(\beta/d^*)^2 = \varepsilon^{-1}\beta/(d^*)^2 + (\eta/2)^2, \quad (1)$$

where ε gives the mean apparent domain size and η is a measure of the strain related with the root mean square strain (e_{rms}) by $e_{rms} \sim \eta/5$ [12]; being β and d^* the integral breath and the reciprocal spacing of every peak, respectively. The graphic representation of Eq. (1) is the so-called Langford plot of the material. As an example, Fig. 7a and b show these plots for apatite-like samples obtained by ball milling at RT for 9 h using as silicon source amorphous silica, and to a portion of this sample after a thermal treatment at 1000 °C for 12 h, respectively. Applying Eq. (1) to the experimental data, and assuming an spherical (isotropic) shape of the domains we obtained the values of the isotropic diameter, $\langle D_{iso} \rangle$, and the root mean square strain, e_{rms}, collected in Tables 1 and 2. From those values, it seems that, as found in other systems [16], the strains induced in the samples as a consequence of milling are difficult to relax; only at high temperature (1000 °C) the strain decreases by one order of magnitude being

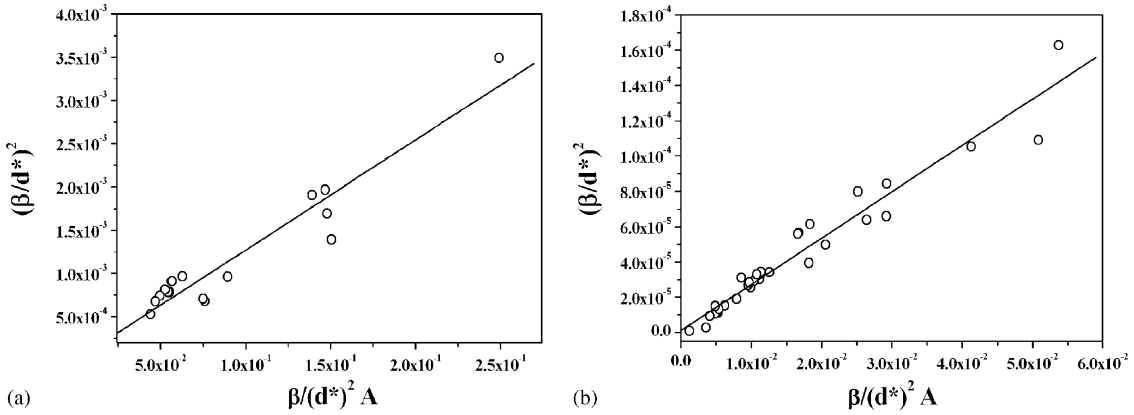

Fig. 7. Langford plots for (a) an apatite-like sample obtained by ball milling at RT for 9 h using amorphous silica as silicon source; and (b) for a portion of the above sample after a thermal treatment at 1000 °C for 12 h.

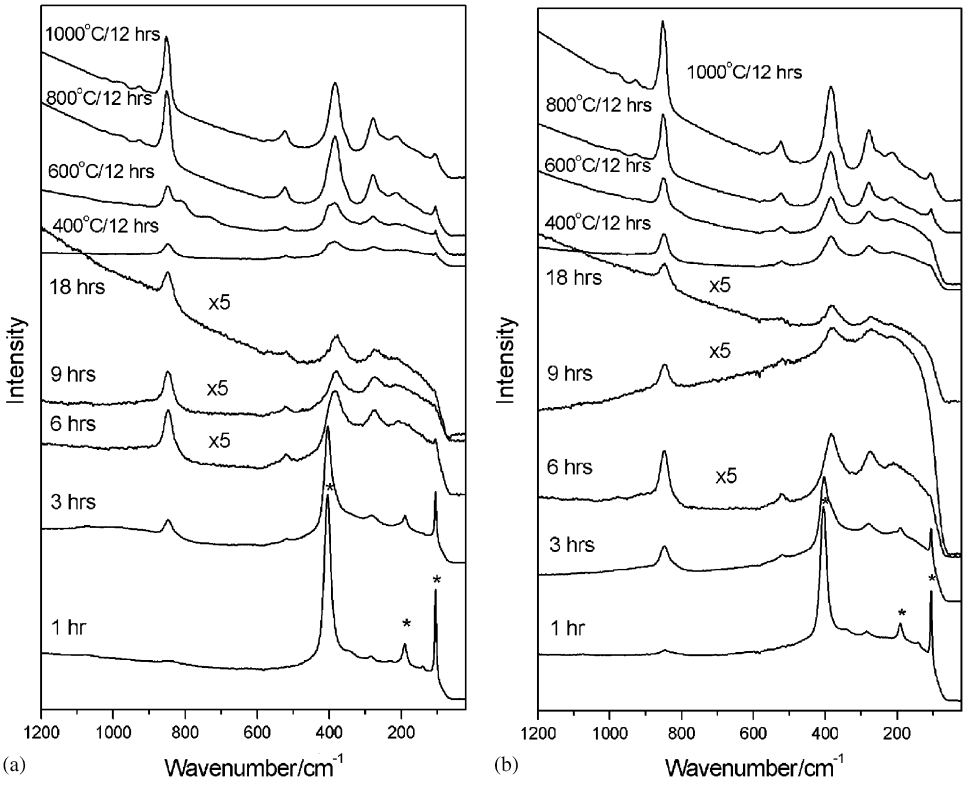

Fig. 8. Raman spectra of samples prepared by milling of A-La_2O_3 and cristobalite (a) or amorphous silica (b). The most characteristic bands of A-La_2O_3 are indicated in the figure by "*".

essentially the same for the as-milled samples and for those treated up to 800 °C. On the contrary, the domain size varies gradually with the temperature of treatment (approximately like an exponential growth as observed for many temperature-activated processes) with activation energies about 26(8) and 52(10) kJ mol^{-1} K^{-1} for the apatites obtained from amorphous silica and low-cristobalite, respectively. These values suggest that the crystallite growth is favored when used amorphous reactant.

In order to complete the structural and microstructural analysis of the as-prepared powder phases and since XRD is not adequate to fully characterize amorphous or poorly crystalline materials, we also examined our samples by using IR and Raman spectroscopies.

3.3. IR and Raman spectra

The measured Raman and IR spectra for the just-milled samples and those milled and thermally treated at different temperatures, are presented in Figs. 8 and 9, respectively. These figures show that after 1 h milling, all the most intense Raman bands at 404, 189 and 105 cm^{-1} as well as

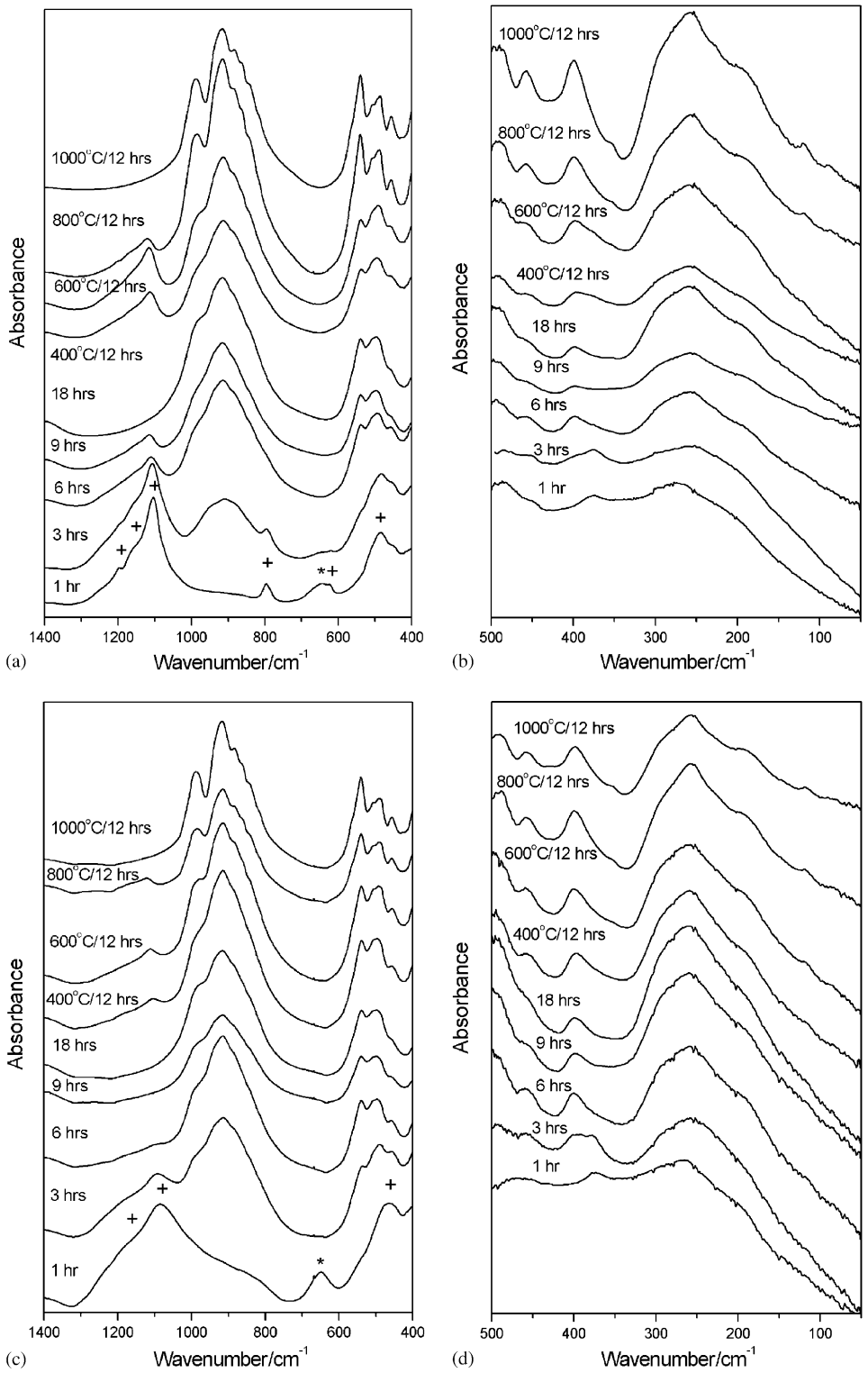

Fig. 9. IR spectra of samples prepared by milling of A-La_2O_3 and cristobalite (a and b) or amorphous silica (c and d). The most characteristic bands of $La(OH)_3$ and SiO_2, are indicated in the figure by "*" and "+", respectively.

IR bands at 1160, 1105, 795 and 484 cm^{-1} can be assigned to either A-La_2O_3 or SiO_2 [17–20]. The presence of IR band near 643 cm^{-1}, which can be assigned to the La–OH bending mode [20,21], indicates that this sample contains also a small admixture of $La(OH)_3$. As the grinding time increases to 3 h, new Raman bands appear near 850 and 380 cm^{-1} as well as IR bands near 915, 540 and 450 cm^{-1}. These bands can be unambiguously assigned to

apatite-type lanthanum silicate [8,22,23]. It is worth noting that the relative intensity of the 915 cm^{-1} IR band (characteristic for the apatite) in respect to the 1105 cm^{-1} band (characteristic for SiO_2) is much higher when sample is prepared from amorphous silica (see Fig. 9). This result shows very clearly that as stated before, the mechanically activated chemical reaction proceeds faster when using amorphous silica as silicon source instead of cristobalite. After milling for 6 h, the samples contain mainly apatite phase but small amount of both SiO_2 and A-La_2O_3 still can be seen. The pure lanthanum silicate phase is obtained after 9 and 18 h of milling when amorphous silica or crystobalite SiO_2 is used, respectively. The measured spectra show that firing the as-prepared lanthanum silicate at temperatures up to 600 °C for 12 h do not produce major changes in the Raman and IR spectra. However, treating the milled powders at 800 and 1000 °C results in intensity increase of some bands and decrease in bands broadening. The most significant changes can be observed for the 988, 539 and 457 cm^{-1} IR bands, and Raman bands observed at 523 and below 280 cm^{-1} (see Figs. 8 and 9). These changes indicate that heat treatment induces some changes in the microstructure of this lanthanum silicate.

Let us now discuss the phonon properties of the lanthanum silicate in detail and the possible origin of observed changes during heat treatment of the prepared samples. Factor group analysis of the hexagonal lanthanum silicate ($P6_3/m$, $Z=2$) shows that the normal modes are distributed among the following irreducible representations: $(12A_g+13E_{2g}+9B_g+8E_{1g}+12B_{1u}+13E_{1u}+9A_u+8E_{2u})$. Since the Si–O bonds are much stronger than the La–O bonds, the crystal structure can be treated as composed of SiO_4 tetrahedra, La^{3+} ions and O^{2-} ions located in large hexagonal tunnels [9] (see Fig. 6). We may, therefore, subdivide the vibrational modes into symmetric stretching modes of SiO_4 group (ν_1: $A_g+E_{2g}+B_{1u}+E_{1u}$), asymmetric stretching modes of SiO_4 group (ν_3: $2A_g+2E_{2g}+B_g+E_{1g}+2B_{1u}+2E_{1u}+A_u+E_{2u}$), symmetric bending modes of SiO_4 (ν_2: $A_g+E_{2g}+B_g+E_{1g}+B_{1u}+E_{1u}+A_u+E_{2u}$), asymmetric bending modes of SiO_4 (ν_4: $2A_g+2E_{2g}+B_g+E_{1g}+2B_{1u}+2E_{1u}+A_u+E_{2u}$), translations of SiO_4 (T: $2A_g+2E_{2g}+B_g+E_{1g}+2B_{1u}+2E_{1u}+A_u+E_{2u}$), librations of SiO_4 (L: $A_g+E_{2g}+2B_g+2E_{1g}+B_{1u}+E_{1u}+2A_u+2E_{2u}$), translations of La^{3+} ions ($3A_g+3E_{2g}+2B_g+2E_{1g}+3B_{1u}+3E_{1u}+2A_u+2E_{2u}$), and vibrations of those oxygen atoms which are located in the channels ($B_g+A_u+E_{2g}+E_{1u}$). From these modes, two modes should be classified as acoustic (A_u+E_u). The A_{1g}, E_{1g} and E_{2g} modes are Raman active and A_u and E_{1u} modes are IR active.

The recorded Raman and IR spectra show the presence of fewer modes than expected (see Figs. 8 and 9 and Table 3) because frequency difference between some modes is small and the corresponding bands are not resolved in the spectra measured of powder samples. The comparison of the measured spectra with that of $Na_{1.5}Sm_{8.5}(SiO_4)_6FO$ [22] shows that the most intense Raman band, observed at 853 cm^{-1}, can be unambiguously assigned, together with a shoulder at 845 cm^{-1}, to symmetric stretching modes of the SiO_4 group. The corresponding IR bands are observed as shoulders at 861 and 842 cm^{-1}. The asymmetric stretching modes of SiO_4 are observed as strong IR bands at 988, 915 and 881 cm^{-1} and from the expected six Raman active asymmetric stretching modes, only one can be observed at 978 cm^{-1}. The comparison of the spectra with literature data allows us also to conclude that the symmetric and asymmetric bending modes of the SiO_4 group are observed in the 383–457 and 485–539 cm^{-1} range, respectively. The assignment of lattice modes is more difficult since a strong coupling between the same symmetry modes is expected. Nevertheless, the comparison of our results with those presented by Toumi et al. [22] for isomorphous $Na_{1.5}Sm_{8.5}(SiO_4)_6FO$ allows us to propose the assignment of modes, which is given in Table 3.

Table 3
Raman and IR wavenumbers observed for the studied samples together with proposed assignment

Raman	IR	Assignment
	1196w	SiO_2
	1160sh	SiO_2
	1105s	SiO_2
978w	988s	ν_3
	915s	ν_3
	881w	ν_3
853s	861sh	ν_1
845sh	842sh	ν_1
	795w	SiO_2
	643w	$La(OH)_3$
	623w	SiO_2
569vw	566sh	?
	539s	ν_4
523w	506w	ν_4
	494sh	?
	485m	ν_4
	484s	SiO_2
404s		A-La_2O_3
	457w	ν_2
383s	399m	ν_2
	374m	A-La_2O_3
353sh	352w	La–O
338w		?
	275s	A-La_2O_3
	290sh	T′(SiO_4) and L(SiO_4)
277m	256s	La–O and T'(SiO_4)
247w	230sh	T′(SiO_4) and L(SiO_4)
213w	196sh	T′(SiO_4) and L(SiO_4)
189w		A-La_2O_3
140vw		?
107w	121w	T′(La)
105m		A-La_2O_3
	90w	T′(La)

w, sh, m, s denotes weak, shoulder, medium and strong, respectively. The bands which do not correspond the lanthanum silicate are written in bold characters. La–O denotes vibrations of the oxygen located in hexagonal tunnels (motions of O_{hex} against La ions).

As mentioned above, the samples subjected to heat treatment show an increase in the intensity of some IR and Raman bands as well as decrease of bandwidths. The bandwidth and intensity changes are especially well visible for the IR bands observed at 988, 539 and 457 cm^{-1} as well as for the 523 cm^{-1} Raman band, assigned by us to stretching and bending modes of the SiO_4 tetrahedra. These changes indicate increase of order with firing temperature. Previous studies of lanthanum silicate samples obtained by a solid-state reaction at high temperatures showed that these materials contain cation vacancies at lanthanum sites [9,24,25]. Since lanthanum ions interact with SiO_4 tetrahedra, the disorder induced by the presence of vacancies at lanthanum sites should influence bandwidth of SiO_4 modes. Neutron powder diffraction studies revealed also that a significant number of oxygen atoms, located in the hexagonal channels, are displaced from the ideal site to a new interstitial site at the periphery of the channels [9,24,25]. It has been shown that when these interstitial oxygen atoms are present, they cause considerable distortion of the nearby SiO_4 tetrahedral units [9,26,27]. It is, therefore, obvious that the presence of interstitial oxygen atoms should also have impact on the bandwidth of SiO_4 bands. Since the heat treatment has no influence on the concentration of cation vacancies, the observed increase of order with increasing temperature can be related to increase in oxygen ion order, possible decrease of interstitial oxygen concentration. If this is the case, our results would indicate that mechanochemical synthesis of lanthanum silicate leads to a large increase in oxygen disorder within hexagonal channels.

4. Conclusions

The preparation of apatite-type lanthanum silicates at room temperature by mechanical milling has been described. The method proposed consists in dry milling in a planetary ball mill at a moderate rotation speed, stoichiometric mixtures of A-La_2O_3 and either amorphous silica or cristobalite SiO_2. The mechanically induced chemical reaction in both cases do not involve the formation of an amorphous precursor as proved by the presence of both lanthanum oxide and the silicate in some of the characteristic XRD patterns, and IR and Raman spectra of the milled powders. As-prepared powder phases are crystalline but present a disordered anion sublattice as proved by IR and Raman data which suggest the presence of interstitial oxygen atoms, decreasing in number as the temperature of post-milling thermal treatment increases. Activation energies for crystallite growth calculated for both silicates from XRD data suggest that the process is favored when amorphous SiO_2 was used as silicon source.

Acknowledgments

This work has been carried out with financial assistance from CONACYT (Grant SEP-2003-C02-44075) and CICYT (Spain) (Project MAT2004-03070-C05-01).

References

[1] J.S. Benjamin, Metall. Trans. 1 (1970) 2943–2951.
[2] S. Nakayama, T. Kageyama, H. Aono, Y. Sadaoka, J. Mater. Chem. 5 (1995) 1801–1805.
[3] S. Nakayama, M. Sakamoto, J. Eur. Ceram. Soc. 18 (1998) 1413–1418.
[4] S. Nakayama, H. Aono, Y. Sadaoka, Chem. Lett. 24 (1995) 431–432.
[5] A.N. Christensen, R.G. Hazell, A.W. Hewat, Acta Chem. Scand. 51 (1997) 37–43.
[6] S. Tao, J.T.S. Irvine, Mater. Res. Bull. 36 (2001) 1245–1258.
[7] S. Celerier, C. Laberty-Robert, F. Ansart, C. Calmet, P. Stevens, J. Eur. Ceram. Soc. 25 (2005) 2665–2668.
[8] G. Tzvetkov, N. Minkova, Mater. Lett. 39 (1999) 354–358.
[9] L. León-Reina, E.R. Losilla, M. Martínez-Lara, S. Bruque, M.A.G. Aranda, J. Mater. Chem. 14 (2004) 1142–1149.
[10] J. Rodriguez-Carvajal, Physica B 192 (1993) 55–69 (see also a report in CPD of IUCr, News letter 26 (2001) 12–19; available at http://www.iucr.org/iucr-top/comm/cpd/Newsletters. The program and manual can be found at http://www-llb.cea.fr/fullweb/powder.htm).
[11] J.I. Langford, NIST Special Publication 846, Proceedings of the International Conference on "Accuracy in Powder Diffraction II", Gaithersburg, MD, USA, 1992.
[12] J.I. Langford, in: P. Snyder, F. Fiala, H. Bunge (Eds.), Defect and Microstructure Analysis by Diffraction, IUCr Monographs on Crystallography, vol. 10, Oxford University Press, Oxford, 1999, p. 59–81.
[13] D. Louër, in: P. Snyder, F. Fiala, H. Bunge (Eds.), Defect and Microstructure Analysis by Diffraction, IUCr Monographs on Crystallography, vol. 10, Oxford University Press, Oxford, 1999, p. 671–697.
[14] W.C. Koehler, E.O. Wollan, Acta Crystallogr. 6 (1953) 741–742.
[15] N.C. Halder, C.N.J. Wagner, Adv. X-ray Anal. 9 (1966) 91–102.
[16] A.F. Fuentes, K. Boulahya, M. Maczka, J. Hanuza, U. Amador, Solid State Sci. 7 (2005) 343–353.
[17] R.A. Nyquist, C.L. Putzig, M.A. Leugers (Eds.), The Handbook of Infrared and Raman Spectra of Inorganic Compounds and Organic Salts, Academic Press Ltd, New York, 1997.
[18] J.H. Denning, S.D. Ross, J. Phys. C 5 (1972) 1123–1133.
[19] M. Scheithauer, H. Knözinger, M.A. Vannice, J. Catal. 178 (1998) 701–705.
[20] N. Imanaka, T. Masui, Y. Kato, J. Solid State Chem. 178 (2005) 395–398.
[21] S. Bernal, J.A. Diaz, R. Garcia, J.M. Rodriguez-Izquierdo, J. Mater. Sci. 20 (1985) 537–541.
[22] M. Toumi, L. Smiri-Dogguy, A. Bulou, Ann. Chim. Sci. Mater. 27 (2002) 17–26.
[23] A.N. Lazarev, T.F. Tenisheva, I.A. Bondar, N.A. Toropov, Izv. AN SSSR Ser. Chim. (1963) 1220–1226.
[24] J.E.H. Sansom, D. Richings, P.R. Slater, Solid State Ion. 139 (2001) 205–210.
[25] Y. Masubuchi, M. Higuchi, H. Katase, T. Takeda, S. Kikkawa, K. Kodaira, S. Nakayama, Solid State Ion. 166 (2004) 213–217.
[26] M.S. Islam, J.R. Tolchard, P.R. Slater, Chem. Commun. (13) (2003) 1486–1487.
[27] J.R. Tolchard, M.S. Islam, P.R. Slater, J. Mater. Chem. 13 (2003) 1956–1961.